International Journal of Thermal Technologies
E-ISSN 2277 – 4114

Available at http://inpressco.com/category/ijtt/

Research Article

Influence of the baffle shape on the characteristics of heat transfer in a channel

M.A. Belmiloud†*, N. Sad_Chemloul†and M.B. Guemmour‡

†Department of Mechanical Engineering, Laboratory of Research and Industrial Technology, University Ibn Khaldoun Tiaret, 14000, Algeria
†Department of Mechanical Engineering, University Ibn Khaldoun Tiaret, 14000, Algeria

Accepted 10 Sept 2016, Available online 24 Sept 2016, **Vol.6, No.3 (Sept 2016)**

Abstract

In this study, we numerically simulated of the influence of shape and height of baffle on heat transfer by mixed convection in a channel. The bottom wall of the channel is heated by a constant heat flux, the other walls are adiabatic. The finite volume method is used to solve the governing equations. The Reynolds number Re between 50 and 300. The Grashof number Gr is fixed at 10^4, and the Prandtl number Pr is kept constant 0.71. The results obtained in this study show that the transfer is louder for the low height irrespective of the shape of baffles, in addition, the number of average Nusselt Nu_{av} takes maximum values for the triangular configuration.

Keywords: *Numerical simulation; mixed convection; shapes of baffles, channel*

1. Introduction

Mixed convection heat transfer in ventilated systems continues to be a fertile area of research, due to the interest of the phenomenon in many technological processes, such as the design of solar collectors, thermal design of buildings, air conditioning, and recently the cooling of electronic circuit boards, electronic enclosures, industrial furnaces. The basic nature the problem interaction between the forced external air stream and the buoyancy-driven flow by the heat source. **Habchi and Acharya [1986]** were numerically analyzed the airflow mixed convection in a vertical channel containing an obstacle on one of her supposed heated walls, while the other is considered to be adiabatic or heated. **Huang *et al* [2005]** have a numerical investigation of the laminar forced convection cooling by a channel containing a plurality of heat sources covered by a porous medium. A numerical study of the cooled mixed convection two heat sources mounted in a horizontal channel has done by **Hamouche and Bessaïh [2008].** **Yang *et al* [2010]** have studied numerically the heat transfer by mixed convection in a channel between two parallel inclined plates containing a solid block on the heated bottom wall. **Amit *et al* [2014]** in their search for work have studied the heat transfer and fluid flow characteristics in a channel in the presence of diamond baffle-shaped to a laminar flow regime. **Menni *et al* [2015]** have made a comparative study numeric between two different forms of fins and transverse baffles. **Nuntadusit *et al* [2015]** have experimentally and numerically investigated the influence of different types of baffles on the heat transfer in a channel. Effect of baffle number on mixed convection within a ventilated cavity, this study presented by **Belmiloud and Sad_Chemloul [2015]**. Their results indicated the two provisions of the outlet of the cavity (BB and BT configurations) have a significant influence on the number of average Nusselt whose maximum value is obtained for the BB configuration due to stream lines that are clamped to the hot wall. Gravity has no influence on heat transfer and whatever the number of baffles used. The influence of gravity is observed only for the BT configuration and particularly in the case of a single baffle.

2. Formulation of the problem

The chosen geometry is a channel whose aspect ratio is $A = 5$. It is used two configurations (square baffle and triangular baffle); the baffles are attached to the channel with a ratio of Hb between 0.2 and 0.3. The bottom horizontal wall is heated by a heat flux $Q = 100\,W/m^2$, the other walls are adiabatic. The distance between the inlet and the baffle is $D = 1.25$. The imposed fluid velocity is obtained by the Reynolds number in the range $50 \le Re \le 300$. The Prandtl number Pr is set at 0.71. The reference temperature is considered constant $T_0 = 298.15\ K$. The presentation of the geometry is given by the following figure:

*Corresponding author: **M.A. Belmiloud**

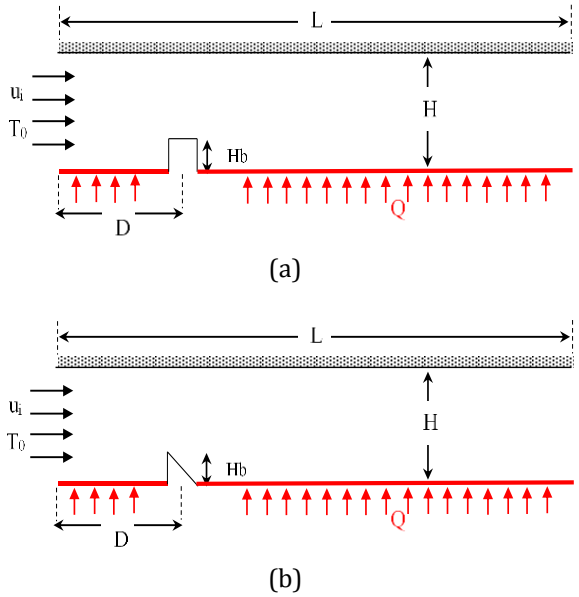

Fig.1 Description of the problem: a) square chicane b) triangular baffle

The general equations of conservation namely, the continuity equation, the equations of movement along x and y and the energy equation are given as follows:

$$\frac{\partial u}{\partial x}+\frac{\partial v}{\partial y}=0 \tag{1}$$

$$u\frac{\partial u}{\partial x}+v\frac{\partial u}{\partial y}=-\frac{\partial P}{\partial x}+\upsilon\left(\frac{\partial^2 u}{\partial x^2}+\frac{\partial^2 u}{\partial y^2}\right) \tag{2}$$

$$u\frac{\partial v}{\partial x}+v\frac{\partial v}{\partial y}=-\frac{\partial P}{\partial y}+\upsilon\left(\frac{\partial^2 v}{\partial x^2}+\frac{\partial^2 v}{\partial y^2}\right)+g\beta\left(T-T_0\right) \tag{3}$$

$$u\frac{\partial T}{\partial x}+v\frac{\partial T}{\partial y}=\alpha\left(\frac{\partial^2 T}{\partial x^2}+\frac{\partial^2 T}{\partial y^2}\right) \tag{4}$$

The dimensionless variables are defined by:

$$x^+=\frac{x}{H},y^+=\frac{y}{H},D=\frac{d}{H},Hb=\frac{h}{H},T^+=\frac{\lambda\left(T-T_0\right)}{QH} \tag{5}$$

To solve the equations Eq (2.2) -Eq (2.4), we consider the following boundary conditions:

At the lower horizontal wall $Q=100\,W/m^2$; u = 0; v = 0

At the upper horizontal wall $Q=0\,W/m^2$; u = 0; v = 0

At the baffle: $Q=0\,W/m^2$; u = 0; v = 0 (6)

At the input of channel: $T_0=298.15K$; $u\neq 0$; v = 0

To determine the characteristics of heat transfer in the steady state, we must take into account the contribution of convection. In this study, the total average Nusselt number is defined as:

$$Nu=\frac{QH}{\lambda\left(T-T_0\right)} \tag{7}$$

3. Numerical Analysis

The resolution of the mass conservation equations, movement and energy are solved by the finite difference algorithm the Semi-implicit method for pressure linked equations SIMPLE. The detail of this method is given by discrete Patankar [1980]. Different equations are discretized in a control volume. The Power law difference scheme (PLDS) used for calculating scalar variables and the quadratic upstream-weighted interpolation for convective kinematics QUICK diagram for scalable variables is presented by Hayase *et al.* [1992]. The convergence of the value considered in this study is:

$$\frac{\left|\varphi_n-\varphi_{n-1}\right|_{max}}{\left|\varphi_n\right|}<10^{-6} \tag{8}$$

Table 1 shows the values of the average Nusselt number Nu_{av} and the dimensionless average temperature T^+_{av} determined in the case of the square and triangular baffle $Hb=0.3$ and to the Reynolds number Re = 100 .Note that for the both configurations, the relative difference Nu_{av} and T^+_{av} obtained is very low. The mesh used in all subsequent calculations is (126X83).

Table 1 shows the effect of mesh on the results for the square configuration and the height baffle Hb = 0.3 , and for Re = 100 .

Mesh	86X63	126X83	Error (% abs)
Nu_{av}	3.1984	3.1964	0.062
T^+_{av}	0.3127	0.3129	0.064

Table 2 shows the effect of mesh on the results for the triangular configuration and the height baffle Hb = 0.3 , and for Re = 100 .

Mesh	86X63	126X83	Error (% abs)
Nu_{av}	3.314	3.309	0.151
T^+_{av}	0.3017	0.3021	0.132

3.1 The code validation

Numerical simulation made using the commercial code ANSYS version.6.3.26 code (FLUENT). For numerical validation of computer code, it is compared our results with those of Figueredo *et al* [1986] and Souza [2006]. The table shows the values of the number of average Nusselt Nu_{av} determined at the cold wall. It is noted that the values of the average Nusselt number Nu_{av} obtained in this study and those obtained by Souza [2006] are very close with a maximum error of 0.996%. However the maximum relative value obtained by Figueredo *et al* [1986] is 4.502%.

Table 3 Number average Nusselt Nu_{av} obtained on the cold wall: comparison between the values of the present study and those of Figueredo *et al* [1986] and Souza [2006]

Gr	Present work	Figueredo *et al* [1986]	% error (abs)	Souza [2006]	% error (abs)
34110	2.941	2.884	1.976	2.912	0.996
60000	3.489	3.468	0.605	3.456	0.955
100000	4.074	4.160	2.067	4.038	0.891
136430	4.475	4.686	4.502	4.440	0.788

4. Results and discussion

4.1 Stream lines distribution

The stream lines obtained by numerical simulation for different cases: shapes of baffles (square baffle and triangular baffle), the heights baffles and the variation of the Reynolds number Re are represented respectively in Figures 2, 3 and 4. Note that the size and location of the vortex region are significantly affected by the geometry of the baffle. Fig. 2 shows the effect of the variation in the shape of baffle. The size of the vortex to the triangular baffle is greater compared to that of the square baffle. This shows that the exchange surface between the current lines and the hot wall is smaller. The influence of the variation in the height of the vortex size is illustrated by Fig.3 for the Reynolds number $Re = 100$ in the case of the square shape of the baffle. The result obtained show that increasing the height of the baffles causes the size of the vortex and thereafter decreasing the exchange surface. Fig. 4 shows the influence of the variation in the Reynolds number Re of the flow recirculation zone to the baffle plate is square and the values of the Reynolds number $Re = 100$ and $Re = 300$. The result shows that the size of the vortices increases with increasing Reynolds number Re.

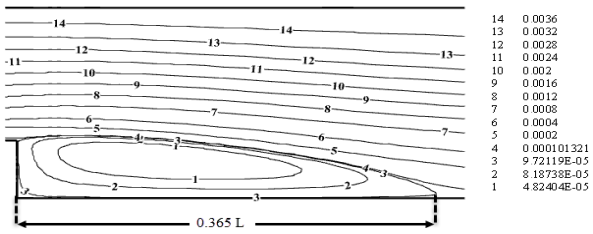

(a)

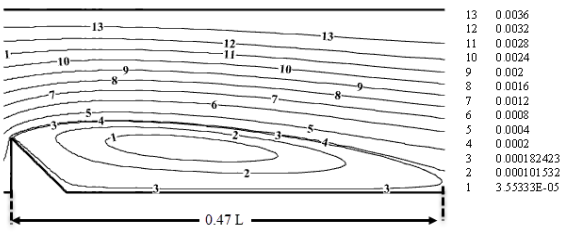

(b)

Fig.2 Shows the variation of the velocity contour for $Re = 200$ and $Hb = 0.3$; a) square configuration; b) triangular configuration

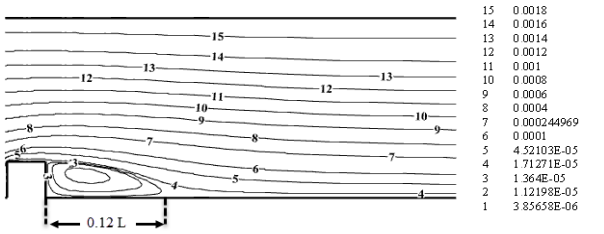

(a)

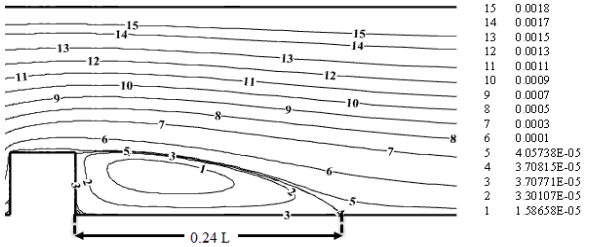

(b)

Fig.3 Shows variation of the velocity contour for $Re = 100$ and the square configuration; a) $Hb = 0.2$; b) $Hb = 0.3$

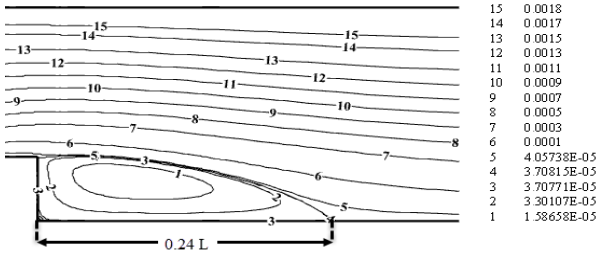

(a)

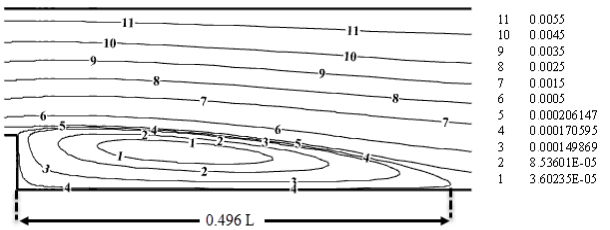

(b)

Fig.4 Shows variation of the velocity contour for the square configuration with $Hb = 0.3$: a) $Re = 100$; b) $Re = 300$

4.2 Nusselt number variation

Figure 5 shows the variation of the average Nusselt number Nu_{av} as a function of the Reynolds number Re for two heights of baffle Hb and for the both configurations of baffle. Note that the average Nusselt number Nu_{av} increases with the increase of Reynolds number whatever shape or height of the baffle. In addition, for the two configurations, the maximum

values of the average Nusselt number Nu_{av} are obtained for the baffle height $Hb = 0.2$.

The average Nusselt number Nu_{av} decreases as the height increase baffle.

The comparison between the two configurations (square and triangular baffle), shows that the heat transfer is best for the triangular chicane, this is due to the flow velocity and size of the vortex caused after the chicane.

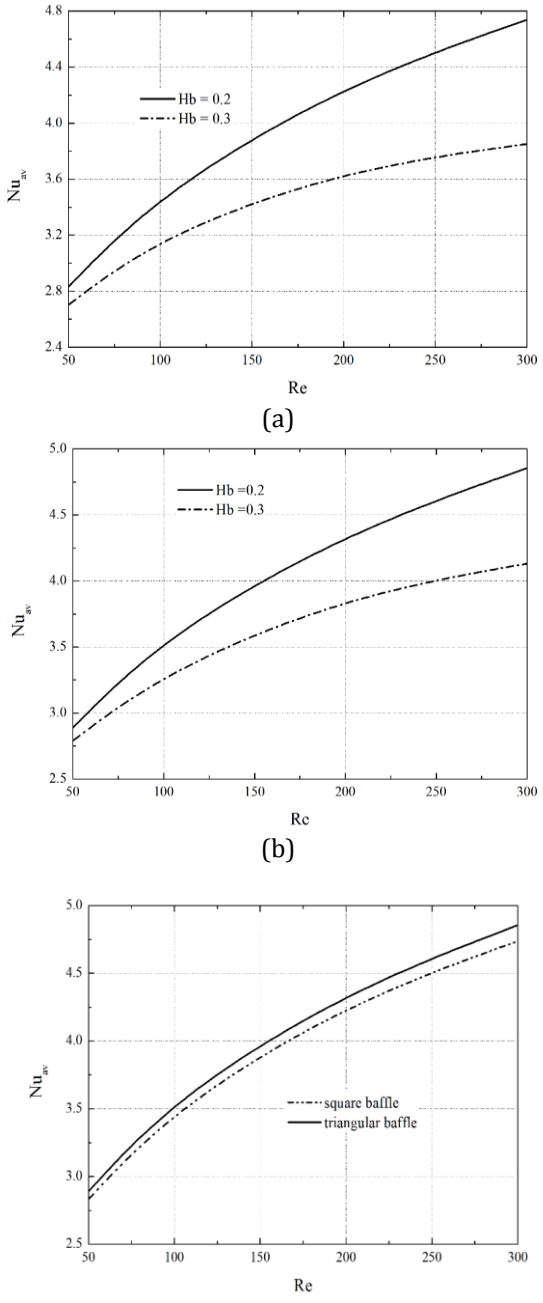

Fig.5 Variation of the Nusselt number Nu_{av} depending on the Reynolds number Re : a) square baffle, b) triangular baffle and c) Comparison between the two configurations for $Hb = 0.2$

4.3 Profile of the temperature

The variation of the average dimensionless temperature T_{av}^{+} as a function of the Reynolds number Re for the two heights of square and triangular baffle are illustrated in Fig. 6. The results obtained show that the average dimensionless temperature T_{av}^{+} decreases with increasing Reynolds number Re irrespective the shape or the height of baffle. The maximum value of the average temperature T_{av}^{+} is obtained for the baffle height.

The comparison between the two configurations shows that for the same Reynolds number Re, the average dimensionless temperature T_{av}^{+} is greater in the case of the square configuration. This may be due to the size of vortex just after the baffle. Indeed , from Fig. 2 the size of the vortex in the case of the triangular baffle is greater compared to that of the square baffle, in other words, the heat exchange surface in the case of the triangular baffle is greater compared to that of the square baffle.

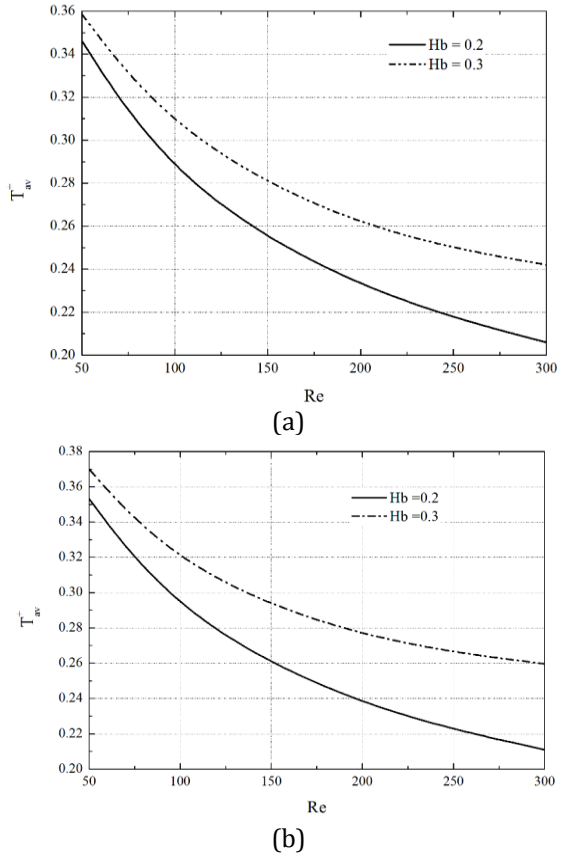

Fig.6 Variation of the profile of the average temperature T_{av}^{+} as a function of the Reynolds number Re : a) square baffle, b) triangular baffle

4.4 Velocity Profiles

Figure 7 shows the variation of profile of the velocity component v as a function of Reynolds number Re and

$Hb = 0.3$ for the both configurations. In this article, only the results obtained at the position $y^+ = 0.5$ are presented.

It is noted that the velocity v increases with increasing Reynolds number Re and shape of the baffle. The maximum value of the velocity is obtained before the baffle in both cases. The comparison between the two configurations shows that for low Reynolds number $Re \leq 100$, the velocity values v almost equal. The highest values v are obtained in the case of the triangular configuration for $Re > 100$.

Figure 8 shows the variation of the v_velocity component profile along x^+ for the different positions y^+ in the case of two configurations and $Hb = 0.3$. Note that the maximum value of the velocity is obtained for the square configuration and upstream of the baffle for the position $y^+ = 0.3$. The results show that for the triangular configuration, the velocity component profiles v for $y^+ = 0.5$ and $y^+ = 0.7$ are almost coincident, and the maximum values are obtained at the position $y^+ = 0.3$.

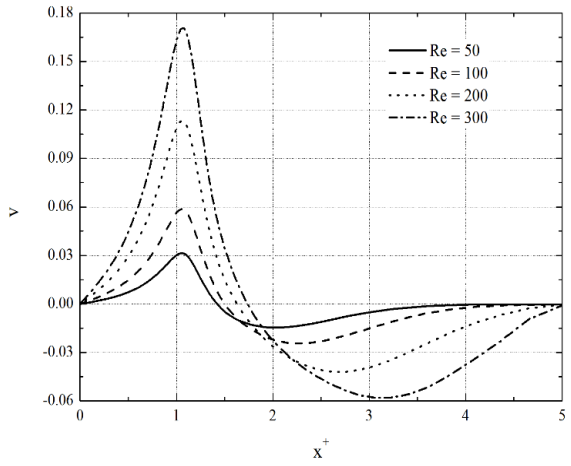

(a)

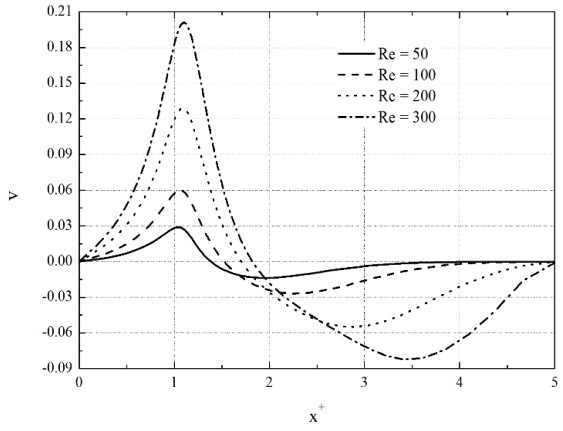

(b)

Fig.7 Shows variation of profile of the velocity component v along x^+ for different values of the Reynolds number Re : a) square baffle, b) triangular baffle

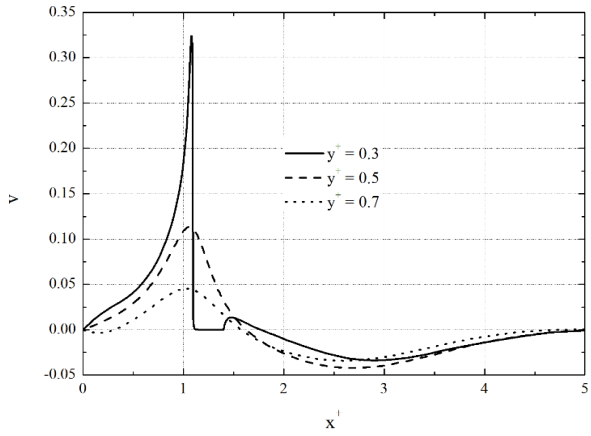

(a)

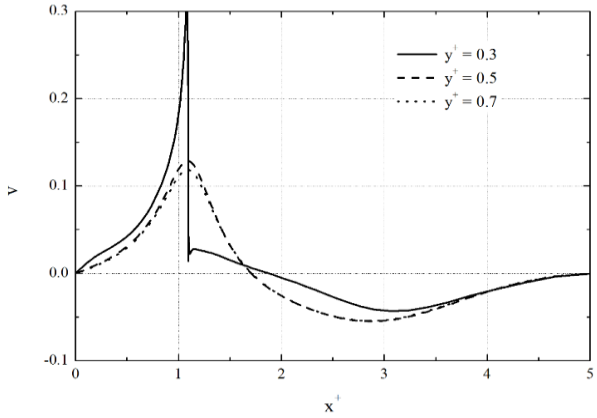

(b)

Fig.8 Shows variation of profile of the velocity component v along x^+ for different position y^+ and for $Re = 200$: a) square baffle, b) triangular baffle.

Figure 9 shows the profile of variation of the u _velocity component along y^+ for $x^+ = 1.5$ and for varying heights Hb. It is noted that for $Hb = 0.2$ and $Re = 200$, the profiles of the component of the velocity u of the two configurations are almost merged below the baffle. At the downstream of the baffle, the velocity changes of direction, a distance of 0.25 L for the square configuration and a distance of 0.28 L for the triangular baffle.

For $Hb = 0.3$ and $Re = 200$, the profile of the velocity component u of the triangular baffle is slightly offset from that of the square baffle to almost their combined maximum velocity for the triangular baffle. At the downstream of the baffle, the velocity changes of direction, a distance of 0.365 L for the square configuration and a distance of 0.47 L for the triangular baffle.

Note that the maximum value of the velocity is obtained for, in other words it increases when the height of the baffle increases.

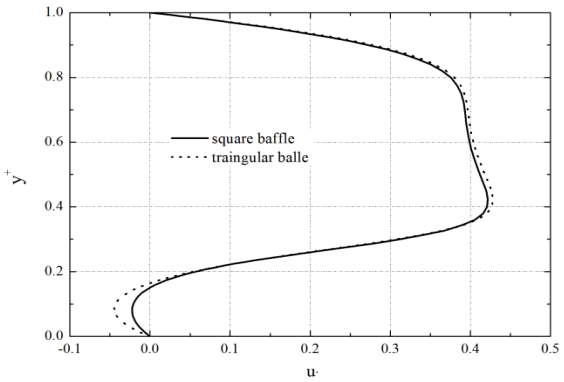

(a)

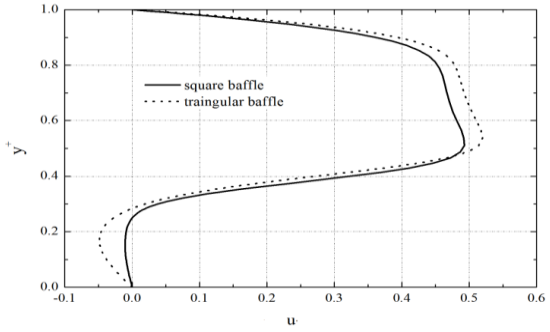

(b)

Fig.9 Shows variation of the velocity component u along y^+ for the position $x^+ = 1.5$ and for $\mathrm{Re} = 200$: a) $\mathrm{Hb} = 0.2$, b) $\mathrm{Hb} = 0.3$.

Conclusion

In this study, we analyzed, the effect of the shape and height of the baffle on the mixed convection in a channel. According to the results we concluded that:

1) The average Nusselt number increases with increasing Reynolds number irrespective of the form of baffle.
2) The average number of Nusselt decreases with increasing height baffles whatever the form of chicane.
3) The average dimensionless temperature decreases as the Reynolds number increases. The values of the velocity component increases with increasing.
4) The comparison between the two configurations shows that good heat transfer is obtained for the triangular configuration.

Nomenclature

A	Aspect ratio of the cavity L/H
D	The distance between the inlet and the baffle
g	Acceleration of gravity
Gr	Grashof number
H	Channel height
Hb	Relative height of baffle
Nu	Nusselt number
Pr	Prandtl number
Q	Heat flux
T	Fluid temperature
T_0	Reference temperature
u_i	Velocity inlet
u, v	Velocity components
x, y	Cartesian coordinates

Symbols Greeks

α	Thermal diffusivity of fluid
β	Coefficient of thermal expansion of the fluid
υ	Kinematic viscosity
λ	Thermal conductivity

Indices and exhibitors

+	Dimensionless values
av	Average

References

S. Habchi and S. Acharya, (1986), Laminar mixed convection in a partially, blocked vertical channel, *International Journal of Heat and Mass Transfer*, vol. 29, pp. 1711-1722.

P. Huang, C. Yang, J. Hwang, M. Chiu, (2005), Enhancement of forced-convection cooling of multiple heated blocks in a channel using porous covers, *International Journal of Heat and Mass Transfer*, vol. 48, pp 647-664.

A. Hamouche, R. Bessaïh, (2008), Mixed convection air cooling of electronic components mounted in a horizontal channel, *International Journal of Theoretical and Applied Mechanics*, vol. 3, pp. 53-64 .

M .Yang, R. Yeh, J. Hwang, (2010), Mixed convective cooling of a fin in a channel, *International Journal of Heat and Mass Transfer*, vol. 53, pp. 760-771.

G. Amit, D Sunil, S. Gurjeet, (2014), CFD analysis of laminar heat transfer in a channel provided with baffles: comparative study between two models of baffles: diamond-shaped baffles of different angle and rectangle, *International Journal of Enhanced Research in Science Technology & Engineering*, pp .267-276.

Y. Menni, A. Azzi et C. Zidani, (2015), Etude numérique comparative entre deux types de chicanes et ailettes (rectangulaire et rectangulaire arrondie) utilisées pour améliorer les performances des capteurs solaires plans à air , *Université Abou Bakr Belkaid Tlemcen*, Algérie.

C. Nuntadusit, I . M. Piya, Wae-hayee, S . Eiamsaard, (2015), Heat transfer characteristics in a channel fitted with zigzag-cut baffles, *Journal of Mechanical Science and Technology*, 29 (6), pp 2547-2554.

M. A. Belmiloud, N. Sad_Chemloul, (2015), Effect of baffle number on mixed convection within a ventilated cavity, *Journal of Mechanical Science and Technology*, 29,11, 4719~4727.

S. V. Patankar, (1980), Numerical heat transfer and fluid flow, *Hemis phere/McGraw-Hill, Washington D.C* .

T. Hayase, J. C. Humphrey and R. Greif, (1992), A consistently formulated quick scheme for fast and stable convergence using finite-volume iterative calculation procedures, *J. of Computational. Physics*, 98 (1) 108-118.

J.R. Figueredo, M.M. Ganzarolli and P.I.F. Almeida, (1986), Convecção Natural em Cavidades Retangulares –Solução Numérica. *II Congresso Latino-Americano de Transferência de Calor e Matéria, São Paulo*, 5, 62-73.

J.J. Souza, 2006, Simulação Numérica da Transferência de Calor por Convecção Forçada, Natural e Mista numa Cavidade Retangular. *M. S. Thesis, Federal University of Itajubá, Itajubá.*